Journal of King Saud University – Science 34 (2022) 102096

Contents lists available at ScienceDirect

Journal of King Saud University – Science

journal homepage: www.sciencedirect.com

Original article

Size dependent antimicrobial activity of *Boerhaavia diffusa* leaf mediated silver nanoparticles

M. Amalin Sobi [a,1], D. Usha [a], M. Umadevi [b], M.R. Bindhu [c,*], Shanmugam Sureshkumar [d], Munirah Abdullah Al-Dosary [e], Hissah Abdulrahman Alodaini [e], Ashraf Atef Hatamleh [e]

[a] Department of Physics and Research Centre, Women's Christian College, Nagercoil, Affiliated to Manonmaniam Sundaranar University, Abishekapatti, Tirunelveli, Tamilnadu, India
[b] Department of Physics, Mother Teresa Women's University, Kodaikanal, Tamil Nadu, India
[c] Department of Physics, Sree Devi Kumari Women's College, Kuzhithurai-629163, Tamilnadu, India
[d] Department of Animal Resource & Science, Dankook University, Cheonan-si, Chungnam, South Korea
[e] Department of Botany and Microbiology, College of Science, King Saud University, P.O. Box 2455, Riyadh 11451, Saudi Arabia

ARTICLE INFO

Article history:
Received 21 February 2022
Revised 20 April 2022
Accepted 11 May 2022
Available online 21 May 2022

Keywords:
Boerhaavia diffusa
Silver nanoparticles
Spherical
Antibacterial
Salmonella typhi

ABSTRACT

Antibacterial activities of *Boerhaavia diffusa* leaves (BDL) mediated silver nanoparticles (AgNPs) were studied. UV–visible spectroscopy (UV–vis), transmission electron microscopic (TEM), X-ray diffraction (XRD) and Energy-Dispersive X-ray spectroscopy (EDS) studies of the synthesized nanoparticles were analyzed too. As the concentration of *Boerhaavia diffusa* leaf (BDL) extract increases, a full width half maximum value decreased and blue shift observed from 427 to 420 nm in the UV–vis spectrum. The XRD confirmed the nanoparticles' high crystallinity and the average nanoparticle size calculated was 14 nm. TEM result reveals that the AgNPs are spherical in shape and the particle sizes range from 6.33 nm to 24.9 nm. The average size of AgNPs was determined to be 13.27 nm which is close to the particle size determined by XRD. EDS shows a prominent peak at 3 kev, indicating that elemental silver is a major component in the reaction medium. The produced nanoparticles were well dispersed and almost spherical in shape. The silver nanoparticles produced at higher concentration of BDL extract against Gram negative pathogen *Salmonella typhi*, showed higher zone of inhibition (23 mm) compared to *Staphylococcus aureus* (21 mm). This biosynthetic method for generating silver nanoparticles prepared in the present work has discrete compensations over chemical reduction synthesis procedures, including great biosafety, ecofriendliness and nontoxicity to the environment.

1. Introduction

Noble metal nanoparticles have established numerous interests according to their interesting applications in biological, chemical, physical, medical and materials science (Kelly et al., 2003; Lee and El-Sayed, 2006; Mani et al., 2021; Qi et al., 2004; Tripathy et al., 2010; Yamanaka et al., 2005). Silver nanoparticles (AgNPs) have received special attention among various metallic nanoparticles owing to their unique features of strong chemical stability, catalytic, electrical conductivity and antimicrobial activities (Mani et al., 2021b; Mani et al., 2021a). A broad research on AgNPs has revealed their excellent beneficial qualities than other metal nanoparticles such as gold, copper, and palladium (Meydan et al., 2022; Seckin et al., 2022; Göl et al., 2021). In vitro, silver nanoparticles have been shown to the interaction of HIV-1 virus in a size-dependent manner, inhibiting the binding of the virus with the host. AgNPs are widely employed in clothes the food industry cosmetics and sunscreens, and are expected to be the next generation of anti-microbial agents. The antibacterial activity of AgNPs might offer new application in pharmaceutical and medical sciences (Shahverdiet al., 2007). When compared to chemical methods, green synthesis method of AgNPs using bio-reducing agents such as and plants, fungi, bacteria and yeast (Mandal et al., 2006). Biosynthesis methods are reported as nontoxic, cost effective, clean and eco-friendly (Awwad et al., 2013). Microbe-mediated nanoparticle synthesis is not an industrially viable option among the

* Corresponding author.
E-mail address: bindhufm@gmail.com (M.R. Bindhu).
[1] Research scholar (Reg. No: 21213282132007).
Peer review under responsibility of King Saud University.

Production and hosting by Elsevier

https://doi.org/10.1016/j.jksus.2022.102096
1018-3647/

numerous biological approaches for Ag nanoparticle synthesis since it necessitates the maintenance of highly aseptic conditions (Anju et al., 2019; Nithiyavathi et al., 2021; Parasuraman et al., 2019a; Parasuraman et al., 2019b; Sathiyaraj et al., 2021). Plant extracts have the potential to be more favourable than microorganisms for the synthesis of nanoparticles since they are easier to scale up, have less biohazard, and require a more involved technique to maintain cell cultures. Plants offer a better platform for nanoparticle synthesis because they include natural capping agents and are free of hazardous compounds (Yoonet al., 2007).

Because of its reported pharmacological effects such as anticonvulsant (Devadigaet al., 2015), antilymphoproliferative (Bose and Chatterjee, 2016) and immunosuppressive (Espentiet al., 2016), *Boerhaavia diffusa* leaves (BDL) were chosen among other plant leaves for the bioreduction of silver and the preparation of stable particles and its antimicrobial activity. *Boerhaavia diffusa* is a distributed perennial herbaceous creeping plant native to India that belongs to the *Nyctaginaceae* family. It's a widely distributed plant that can be found in India, the Pacific and the southern US. Punarnava is the name given to *Boerhaavia diffusa* in India. Punarnavine, a plant alkaloid, has been demonstrated to have anti-estrogenic, anti-cancer, immune-modulatory and anti-amoebic properties.

In many regions of India, BDL is commonly consumed as a green vegetable, and its therapeutic qualities are well known. The ancient use of the plant includes relieving problems like hysteria, epilepsy, gastritis, fever, jaundice, convulsion, dysentery, asthma, diarrhea, pain relief and to improve eyesight (Huang et al., 2020). The presence of phenolic glycosides, methyl flavone, and rotenoids such as Boeravinone-A, Boeravinone-B, Boeravinone-M, Coccineone-B, 6-O-Demethylboeravinone, and 2′-O-methylabroni soflavone was confirmed by phytochemical screening of BDL (West, 1974). In this study, we report small spherical shaped silver nanoparticles by BDL extract and characterization of the prepared NPs by UV–vis, XRD, EDS and TEM. The anti-bacterial activities of the prepared AgNPs were analysed too.

2. Experimental

2.1. Material and methods

Analytical grade of silver nitrate ($AgNO_3$) was received from Sigma-aldrich chemicals. *Boerhaavia diffusa* were collected from our college campus, Kuzhithurai, Tamilnadu.

2.2. Preparation of Boerhaavia diffusa leaves (BDL) extract

100 g of BDL were added with 250 ml of distilled water at 100 °C for 20 min. Then the extract was subjected to centrifugation (1000 rpm) and filtered by Whatman No.1 filter paper. The obtained pale-yellow coloured extract was collected for the preparation of AgNPs and their characterizations.

2.3. Green synthesis of AgNPs

5 ml extract of BDL was added with $AgNO_3$ (5 mM) and were subjected to stirring at 30 °C. Rapid reduction that has taken place were confirmed by the appearance of brownish coloured solution. This Ag solution was noted as D1. Colloids D2 and D3 were synthesized by adding 10 and 15 ml of BDL extract with $AgNO_3$ (5 mM) in the same procedure. D1, D2 and D3 were stable for six months without showing any precipitation. The prepared solutions were subjected to drying process at 100 °C. The dried powders of D1, D2 and D3 were taken for UV–vis, XRD and TEM characterizations.

2.4. Characterizations

The production of AgNPs was studied using UV–visible spectral spectroscopy by Shimadzu spectrophotometer (UV 1700). The X-RD pattern was analysed by PANalytical X'pert PRO diffractometer worked at 40 kV/30 mA by Cu Kα radiation. TEM images were done by JEOL-TEM-2010 HR-TEM worked at 200 kV.

Disc diffusion method was used to estimate anti-bacterial action of Ag-NPs derived from BDL to fight bacteria namely *Staphylococcus aureus* and *Salmonella typhi*. All samples were inoculated into sterile nutrient broth (Hi Media) (5 ml). And they were incubated for 3 to 5 h to normalize the culture into (106 CFC/ml) McFarland-standards. 3 repeats of individual organism was organized by dispersing 100 µl of rejuvenated culture on Mueller-Hinton-Agar/Hi Media by a spreader. 50 µl samples of silver nanoparticles derived from BDL were added in one well (7 mm-diameter). All the petri-plates were reserved in the incubator at 37 °C for 1 day for organism in which their antimicrobial action was indicated with zone of inhibition in mm.

3. Results and discussion

3.1. UV–vis studies

Fig. 1(a) shows the UV–vis spectra of time variation (1 min-7 hr) study of D3. The stability of the nanoparticles was confirmed by its optical spectra recorded at different time, as it's a vital factor in the preparation of nanoparticle. As illustrated in Fig. 1, the surface plasmon resonance (SPR) bands of the produced colloids blue shifted with increased absorbance as a result of reaction duration. Furthermore, as the reaction time grew, the intensity of the surface plasmon resonance peak rose, indicating that the silver ions continued to be reduced and the concentration of Ag-NPs increased (Bohren and Huffman,1998). It was discovered that as the reaction time increases, the peak grows sharper. The creation of AgNPs began in less than a minute and continued for up to 7 h, with only minor variations after that. Since small sized metal nuclei grow and consume metal ions at the same time, the availability of a higher number of nuclei causes the particle size to drop after 7 h of reaction. Initially, the prepared nanoparticles become colorless and turned into brown coloured silver nanoparticles, after that they showed any changes in the color indicating complete reduction. The position of the surface plasmon peaks and the color of the solutions remain stable for a month and didn't show any sign of aggregation. The battle between electrostatic repulsion and weak Van der Waals forces of attraction results a potential barrier, which leads to stability.

Fig. 1(b) shows the UV–vis spectra of D1, D2 and D3. It displays the surface plasmon peak of D3 becomes sharper with a higher concentration of BDL extract. The position of the plasmon absorption exhibit a blue shift depends upon the particle shape, size, surrounding dielectric medium and the state of aggregation (Azizian-Shermehet al., 2017). When increasing the concentration of BDL extract in the reaction medium, a full-width half maximum value of the the plasmon absorption decreases and the blue shift is observed from 427 to 420 nm, and it indicates smaller sized particles. The homogeneous distribution of spherical particles is confirmed by the sharp narrow blue shifted plasmon absorption of D3.

3.2. XRD studies

Fig. 2 shows that the XRD pattern of D1, D2 and D3. The diffraction peaks are observed at 38.08°, 44.29°, 64.4° and 77.33° are indexed as (111), (200), (220) and (311) reflections of face centered cubic structure of silver (JCPDS file no. 04–0783). Three other

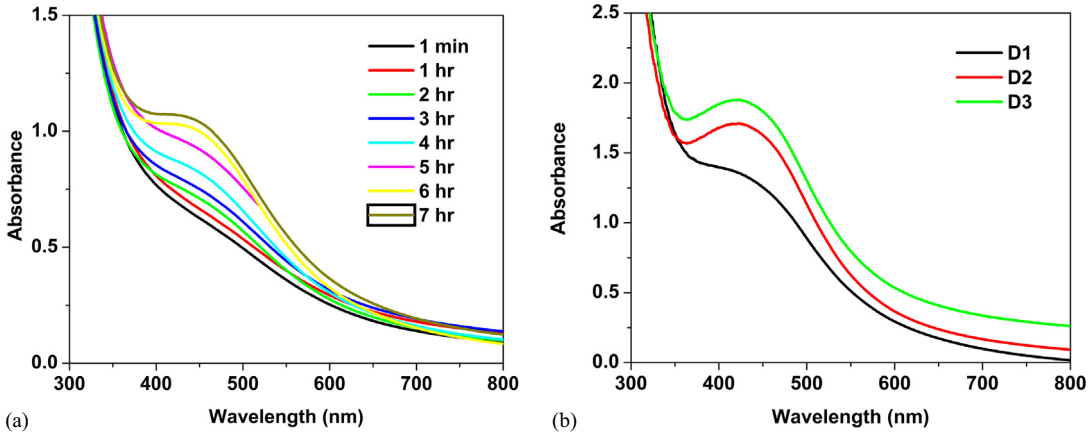

Fig. 1. UV–vis spectra of (a) time variation study of D3 and (b) D1, D2 and D3.

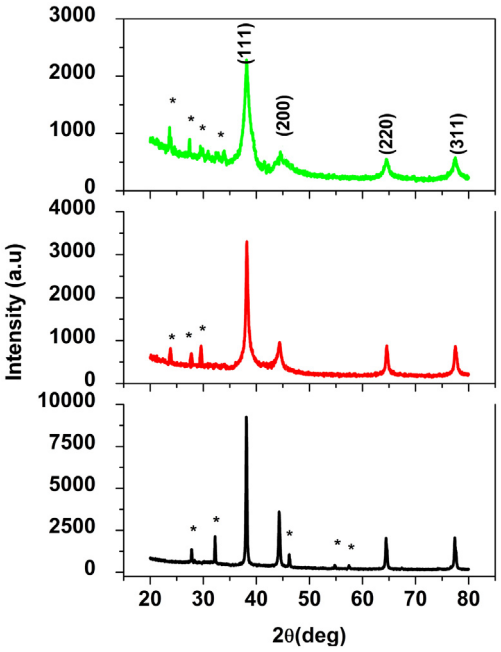

Fig. 2. XRD pattern of D1, D2 and D3.

peaks are at 27.8°, 32.1° and 46.2° indicate the existence of ascorbic acid in the BDL extract (JCPDS file no. 22–1560 and 22–1532). The reduction of intensity of these extra peaks compared to silver, indicating Ag is the primary ingredient in the reaction medium.

The average size, cell volume and lattice parameter of D1, D2 and D3 are tabulated in Table 1. All these structural parameters are matching to the JCPDS: 04–0783. It can be seen that the broadening of peaks indicates that the D3 has very small crystalline sizes (Jenkins and Snyder,1996). The average size of the particles gets reduced when increasing the concentration of BDL extract.

3.3. TEM studies

TEM images of D3 derived from higher concentration of BDL is shown in Fig. 3a and b. TEM analysis explicates the size and morphology of the obtained particles. It reveals that the AgNPs are spherical shaped and the sizes range from 6.325 nm to 24.9 nm. The average particle size of AgNPs is determined to be 13.268 nm which is close to particle size determined by XRD.

Table 1
Average size, volume and lattice parameter of D1, D2 and D3.

Sample	Average size (D) (nm)	Volume (V) $(Å)^3$	Lattice parameter (a) (Å)
D1	27	68.267	4.0870
D2	18	68.242	4.0865
D3	14	68.222	4.0861

Vijaya kumar et al. have reported 25 nm sized BDL extract mediated AgNPs (Vijay Kumara et al., 2014). The SAED pattern of D3 shown in Fig. 3c confirmed its crystalline nature. And it is verified by the intense circular spots assigned to (111), (200), (220) and (311) planes.

3.4. EDS studies

EDS is used to confirm the elemental composition and purity of the particles. Fig. 3d shows a prominent peak at 3 kev, indicating that silver is a major constituent. The copper substrate is responsible for the Cu signal. The existance of carbon and oxygen in the produced nanoparticles is designated by the development of C and O signals.

3.5. Antimicrobial activity

Bacterial resistance to standard medical techniques is on the rise around the world, posing a severe threat to human health. Owing to the haphazard utilization of anti-microbial medications, microorganisms have developed resistance to many antibiotics, causing clinical issues in the treatment. In light of the rising frequencies of illnesses with growing multidrug resistance, clinicians have few options for treating such infections. The usage of plasmonic nanoparticles is the effective way to overcome the bacterial resistance. Nanoparticles have a larger contact area with the pathogens due to their high surface area to volume ratio and smaller particle size. This trait increases biological as well as chemical activities of the particles with strong antimicrobial efficacy. Ag is a benign metal that can kill over 650 types of disease causing germs. It is being employed for water purification treatment (as a bactericide) and also to avert the upsurge of algae and bacteria in water filters. AgNPs are used to kill bacteria in textiles, polymers, medical devices, burn dressings and dental materials. The anti-microbial activity of D1, D2 and D3 was deliberated upon Gram-positive pathogen *Staphylococcus aureus* and Gram negative pathogen *Salmonella typhi*. The zone of inhibition of D1, D2 and

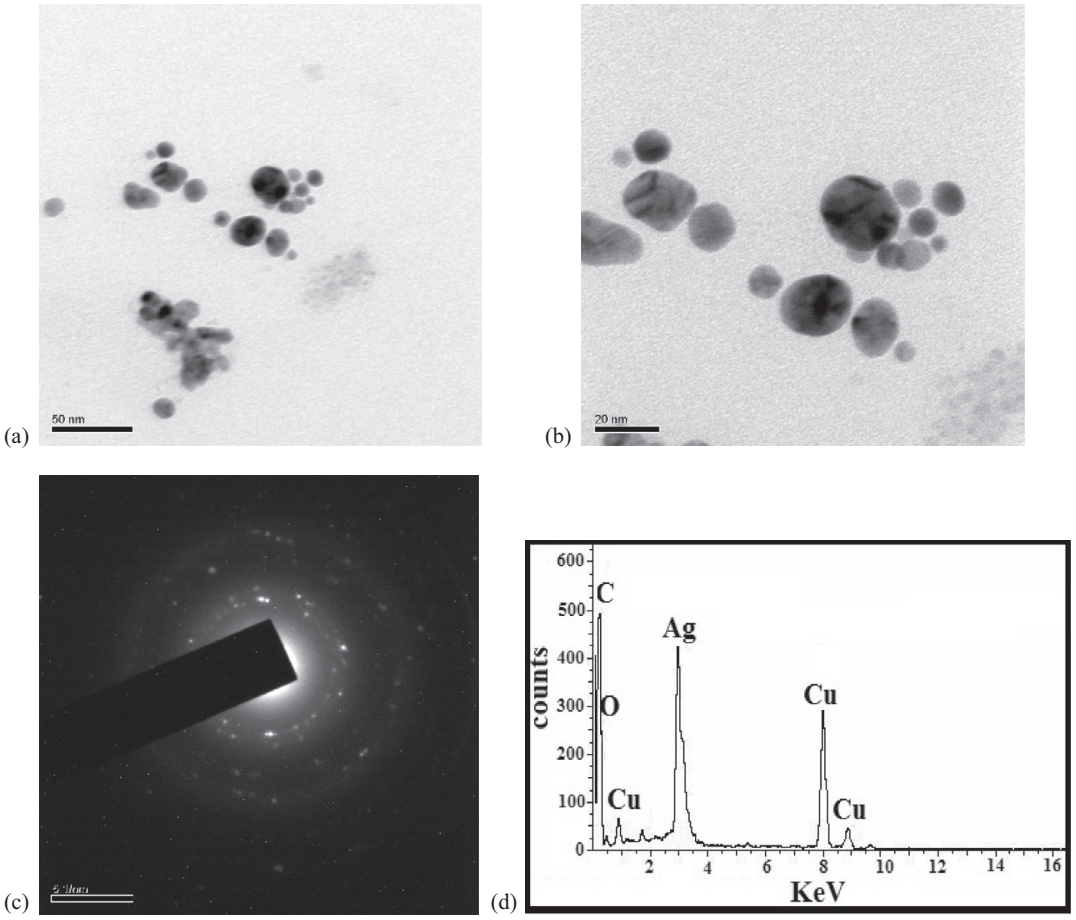

Fig. 3. TEM images (a-c) and EDS spectrum (d) of D3.

D3 against (a) *Salmonella typhi* and (b) *Staphylococcus aureus* is shown in Fig. 4. Prasad et al have reported the antimicrobial activity of silver nanoparticles synthesized by *Moringa oleifera* leaf extract against *S.aureus*, *C.krusei*, *K.pneumonia* and *C. tropicalis* with 6 mm to15 mm of inhibion zones (Prasad and Elumalai, 2011). The zone of inhibition of *Moringa Oleifera flower* assisted AgNPs have been reported as the range lies between 9 mm and 11 mm for *S.aureus*, *S.paratyphi*, *K.pneumoniae*, *P.aeruginosa*, *M.luteus* and *B.subtilis* (Kalaiselvi et al., 2018). It has been reported as the inhibion zones with 29 mm and 17 mm was observed for green synthesized AgNPs against and *Staphylococcus aureus* and *Klebsiella pneumonia* respectively (Bindhu et al., 2020). It has been also reported as the inhibition zones of 23 mm was observed for green synthesized AgNPs against *E. coli.* (Vijilvani et al., 2019). The antibacterial activity of the AgNPs prepared by *Solanum trilobatum* bark extract was assessed by using *E. coli, Bacillus* sp., and *A. niger and* the observed inhibition zones lies between 6 mm and 18 mm (Ramanathan et al., 2018). In our case, the D3 against *Salmonella typhi*, showed higher zone of inhibition compared to *Staphylococcus aureus*. The zone of inhibition of D3 is 23 nm for *Salmonella typhi.* Table 2 shows that antimicrobial activity of D3 against various pathogens. This revealed that the size dependent anti-microbial activity of BDL assisted AgNPs. The observed differences in the zone of inhibition are owing to the difference in the susceptibility of dissimilar bacteria to the particles (see Table 2).

Ag-NPs contact to bacteria cause adhesion of nano sized particles to the cell wall as well as its membrane. The positive charged AgNPs gives electrostatic attraction to the negative charged cell membrane of the bacteria, so assists the attachment of AgNPs into the cell membrane. The contact of Ag-NPs with the cell wall causes irrevocably alterations in the cell wall structure ensuing in its disturbance. This has an impact on the lipid bilayer's integrity as well as the cell membrane's permeability. Increased membrane permeability is caused by changes in cell shape, which compromises the cell's capacity to adequately control transport action all the way through the plasma membrane. The cells of microbes exposed to Ag-NPs undergo genetic modification of condensation of hereditary material. Thus, various critical cellular activities are suppressed, leading to cell necrosis and then to decease. *Salmonella typhi* are vulnerable to Ag-NPs than *Staphylococcus aureus*. *Salmonella typhi* is more susceptible to D3 owing to less thick cell wall (3–4 nm), the existence of lipopolysaccharides (LPS) in the cell membrane and less peptidoglycan. Thus the obtained results suggest that Ag-NPs generated in this way have good anti-bacterial action against Gram positive as well as negative bacteria.

The Table. 3 aims to discuss the antimicrobial application of green synthesized AgNPs of similar size and shape of *Boerhaavia diffusa* leaf mediated AgNPs.

4. Conclusion

A biological reducing agent, *Boerhaavia diffusa* leaf extract was used to prepare AgNPs in this study. The prepared nanoparticles were characterized by EDS, UV–vis, XRD and TEM measurements. The average size of AgNPs was 14 nm estimated from Scherer method. The surface plasmon absorption of biosynthesized AgNPs was validated by UV–vis absorbance spectroscopy. The crystalline nature and FCC structure of the nanoparticles was cleared from the XRD. The produced spherical particles are well dispersed in form. Antibacterial activity is observed in the biosynthesized silver

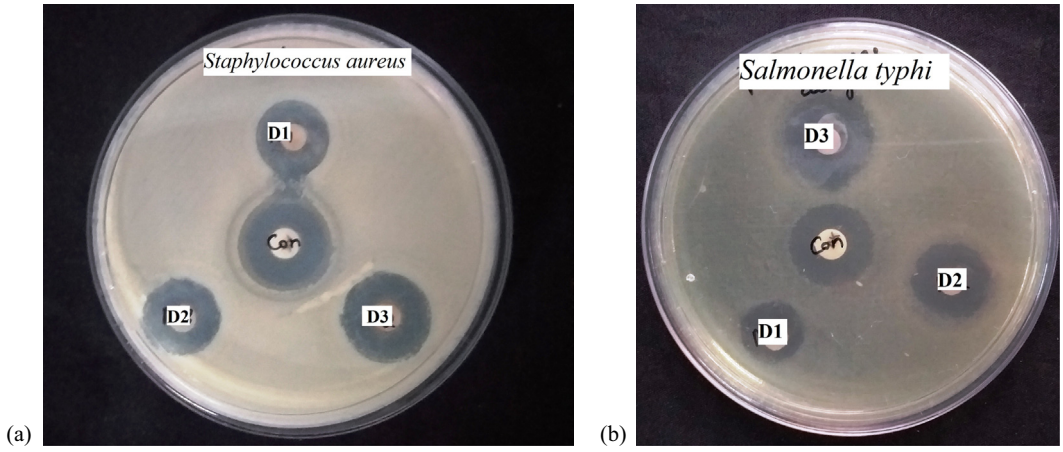

Fig. 4. The zone of inhibition of D1, D2 and D3 against (a) *Salmonella typhi* and (b) *Staphylococcus aureus*.

Table 2
The zone of inhibition of D1, D2 and D3 against *Salmonella typhi* and *Staphylococcus aureus.*

Microorganisms	Zone of inhibition (mm)			
	D1	D2	D3	Control (Amikacin)
Salmonella typhi	15	18	23	20
Staphylococcus aureus	18	20	21	17

Table 3
The size, shape, structure, tested microorganisms & various reducing agent involved in the reduction of AgNPs.

S.No	Reducing agents involved in the reduction of AgNPs	Size (nm)	Shape	structure	Test Microorganisms	Reference
1.	*Amaranthus gangeticus Linn*	11–15	Globular	FCC	*S. flexneri, B. subtilis, Sclerotinia* sp.	(Kolya et al., 2015)
2.	*Pistacia atlantica*	10–50	Spherical	FCC	*S. aureus*	(Devadiga et al., 2015)
3.	*Psidium guajava*	10–90	Spherical	FCC	*P. aeruginosa*	(Bose et al., 2016)
4.	*Terminalia chenbula*	10–30	Spherical	FCC	*E. Coli*, and *B. subtilis*	(Espenti et al., 2016)
5.	*Tamarix gallica*	5–40	Spherical	FCC	*E. coli*	(Lopez-Miranda et al., 2016)
6.	*Maclura pomifera*	6–16	Spherical	FCC	*S. aureus, Bacillus cereus, E. coli, P. aeruginosa, A. niger and C. albicans*	(Azizian-Shermeh et al., 2017)
7.	*Paederia foetida Linn.*	5–25	Spherical	FCC	*B. cereus, S. aereus, E. coli, A. niger*	(Bhuyan et al., 2017)
8.	*Talinum triangularae*	13.86	Spherical	FCC	*S. typhi, E. coli, B. subtilis, C. albicans S.aureus*	(Elemike et al., 2017)
9.	*Lippia citriodora*	10–45	Spherical	FCC	*C. albicans, S. aureus, S. typhi, B. subtilis, E. coli.*	(Elemike, et a., 2017)
10.	*Catharanthus roseus*	10–88	Spherical	FCC	*E. coli, P. aeruginosa, pneumonia, S. aureus*	(Saratale et al., 2018)
11.	*Lavandula × intermedia*	11–47	Spherical	FCC	*F. Oxysporum, B. cereus, S. typhi, K. oxytoca, S. aureus, A. niger, C. albicans*	(Saratale et al., 2018)
11.	*Taraxacum officinale*	5–30	*Spherical*	FCC	*X. axonopodis, P. syringae*	(Saratale et al., 2018)
12.	*Indigofera tinctoria*	9–26	Spherical	FCC	*A. niger, Pseudomonas* sp., *A. fumigatus, E. coli*	(Vijayan et al., 2017)
13	*Tecoma stan*	2–40	Spherical	FCC	*B. subtilis, S. aureus, K. pneumoniae*	(Biswas et al., 2018)
14	*Ligustrum lucidum*	13	Spherical	FCC	*S. turcica*	(Huang et al., 2020)
15	*Carya illinoinensis*	12–30	Spherical	FCC	*E. coli, S. aureus, P. aeruginosa, L. monocytogenes*	(Dalir et al., 2020)
16	*Aspilia pluriseta*	1–20	Spherical	FCC	*C. albicans, B. subtilis, E. coli, S. aureus, P. aeruginosa*	(Nyabola et al., 2020)
17	*Scoparia dulcis*	3–18	Spherical	FCC	*P. aeruginosa, B.subtilis, E. coli, S. aureus, C. albicans, A. niger*	(Parvataneni, 2020)
18	*Milkania micrantha*	10–20	Spherical	FCC	*B. subtilis, E. coli, P. aeruginosa, S. pneumonia*	(Biswas et al., 2019)
19.	*Syzygium cumini*	11–19	Spherical	FCC	*S. aureus, A. flavus, A. parasiticus*	(Asghar et al., 2020)

nanoparticles against a variety of therapeutically significant pathogenic pathogens. Gram-negative bacteria like *Salmonella shigella* were vulnerable to AgNPs than *Staphylococcus aureus*. This simple method of biosynthesis of AgNPs proffers a precious role in biosynthesis and nanoscience evading the existence of harmful and poisonous waste.

Declaration of Competing Interest

The authors declare that they have no known competing financial interests or personal relationships that could have appeared to influence the work reported in this paper.

Acknowledgement

The authors extend their appreciation to the Researchers supporting project number (RSP2021/316), King Saud University, Riyadh, Saudi Arabia.

References

Anju, V.T., Parasuraman, P., Sruthil Lal, S.B., Alok, S., Asad, S., Needa, A.B., Marzouq, H.A., Kaviyarasu, K., Siddhardha, B., 2019. Antimicrobial photodynamic activity of toluidine blue-carbon nanotube conjugate against Pseudomonas aeruginosa and Staphylococcus aureus - Understanding the mechanism of action Photodiagnosis Photodyn. Ther 27, 305–316.

Asghar, M.A., Zahir, E., Asghar, M.A., Iqbal, J., Rehman, A.A., 2020. Facile, one-pot biosynthesis and characterization of iron, copper and silver nanoparticles using Syzygium cumini leaf extract: As an effective antimicrobial and aflatoxin B1 adsorption agents. PLoS One 15. https://doi.org/10.1371/journal.pone.0234964.

Awwad, A.M., Salem, N.M., Abdeen, A.O., 2013. Green synthesis of silvernanoparticles using Carob leaf extract and its antibacterial activity. Int. J. Ind. Chem. 4, 29-35. https://doi.org/10.1186/2228-5547-4-29.

Azizian-Shermeh, O., Einali, A., Ghasemi, A., 2017. Rapid biologically one-step synthesis of stable bioactive silver nanoparticles using Osage orange (*Maclura pomifera*) leaf extract and their antimicrobial activities. Adv. Powder Technol. 173 (28), 3167–3171.

Bhuyan, B., Arijita, P., Paul, B., Dhar, S.S., Dutta, P., 2017. *Paederia foetida* Linn. promoted biogenic gold and silver nanoparticles: Synthesis, characterization, photocatalytic and in vitro efficacy against clinically isolated pathogens. J.Photochem. Photobiol. B. 173, 210–215. https://doi.org/10.1016/j.jphotobiol.2017.05.040.

Biswas, A., Vanlalveni, C., Adhikari, P.P., Lalfakzuala, R., Rokhum, L., 2019. Biosynthesis, characterisation and antibacterial activity of *Mikania micrantha* leaf extract-mediated AgNPs. Micro Nano Lett. 14, 799–803. https://doi.org/10.1049/mnl.2018.5661.

Bindhu, M.R., Umadevi, M., Esmail, Galal Ali, Al-Dhabi, Naif Abdullah, Valan Arasu, M., 2020. Antimicrobial and catalytic activities of biosynthesized gold, silver and palladium nanoparticles from Solanum nigurum leavesGreen synthesis and characterization of silver nanoparticles from *Moringa oleifera* flower and assessment of antimicrobial and sensing properties. J. Photochem. Photobiol. B. 205, 111836.

Biswas, A., Chawngthu, L., Vanlalveni, C., Hnamte, R., Lalfakzuala, R., Rokhum, L., 2018. Biosynthesis of Silver Nanoparticles Using *Selaginella bryopteris* Plant Extracts and Studies of Their Antimicrobial and Photocatalytic Activities. J. Bionanosci. 12, 227–232. https://doi.org/10.1166/jbns.2018.1510.

Bohren, C.F., and Huffman D.R., 1998. Absorption and Scattering of Light by Small Particles. New York: John Wiley & Sons Inc; DOI:10.1002/9783527618156.

Bose, D., Chatterjee, S., 2016. Biogenic synthesis of silver nanoparticles using guava (*Psidium guajava*) leaf extract and its antibacterial activity against *Pseudomonas aeruginosa*. Appl. Nanosci. 6, 895–901. https://doi.org/10.1007/s13204-015-0496-5.

Dalir, S., Djahaniani, H., Nabati, F., Hekmati, M., 2020. Characterization and the evaluation of antimicrobial activities of silver nanoparticles biosynthesized from Carya illinoinensis leaf extract. Heliyon 6, e03624. https://doi.org/10.1016/j.heliyon.2020.e03624.

Devadiga, A., Shetty, K.V., Saidutta, M.B., 2015. Timber industry waste-teak (*Tectona grandis* Linn.) leaf extract mediated synthesis of antibacterial silver nanoparticles. Int. NanoLett. 5, 205–214. https://doi.org/10.1007/s40089-015-0157-4.

Elemike, E.E., Onwudiwe, D.C., Ekennia, A.C., Ehiri, R.C., Nnaji, N.J., . Phytosynthesis of silver nanoparticles using aqueous leaf extracts of Lippia citriodora: Antimicrobial, larvicidal and photocatalytic evaluations. Mater. Sci. Eng. C. Mater. Biol. Appl. 75, 980–989. https://doi.org/10.1016/j.msec.2017.02.161.

Elemike, E.E., Onwudiwe, D.C., Fayemi, O.E., Ekennia, A.C., Ebenso, E.E., Tiedt, L.R., 2017. Biosynthesis, Electrochemical, Antimicrobial and Antioxidant Studies of Silver Nanoparticles Mediated by Talinum triangulare Aqueous Leaf Extract. J. Clust. Sci. 28, 309–330. https://doi.org/10.1007/s10876-016-1087-7.

Espenti, C.S., Rao, K.S.V.K., Rao, K.M., 2016. Bio-synthesis and characterization of silver nanoparticles using *Terminalia chebula* leaf extract and evaluation of its antimicrobial potential. Mater. Lett. 147, 129–133. https://doi.org/10.1016/j.matlet.2016.03.106.

Göl, Fatma, Aygün, Ayşenur, Seyrankaya, Abdullah, Gür, Tuğba, Yenikaya, Cengiz, Şen, Fatih, 2021. Corrigendum to "Green synthesis and characterization of Camellia sinensis mediated silver nanoparticles for antibacterial ceramic applications" Materials Chemistry and Physics 250, (2020), 123037. Mater. Chem. Phys. 270. https://doi.org/10.1016/j.matchemphys.2021.124783.

Hamdullah Seckin Rima Nour Elhouda Tiri, Ismet Meydan, Aysenur Aygun, Meliha Koldemir Gunduz, Fatih Sen, An environmental approach for the photodegradation of toxic pollutants from wastewater using Pt–Pd nanoparticles: Antioxidant, antibacterial and lipid peroxidation inhibition applications Environ. Resear. 208 112708 2022.

Huang, W., Yan, M., Duan, H., Bi, Y., ChengandH, X., 2020. Yu. J. Nanomater. 1–7.

Meydan, Ismet, Burhan, Hakan, Gür, Tuğba, Seçkin, Hamdullah, Tanhaei, Bahareh, Sen, Fatih, 2022. Characterization of Rheum ribes with ZnO nanoparticle and its antidiabetic, antibacterial, DNA damage prevention and lipid peroxidation prevention activity of in vitro. Environ. Resear. 204.

Jenkins, R., Snyder, R.L., 1996. Introduction to X-ray powder diffractiometry. John Wiley and Sons New York 544.

Kalaiselvi, V, Mathammal, R, Vijayakumar, S, Vaseeharan, B, 2018. Microwave assisted green synthesis of Hydroxyapatite nanorods using Moringa oleifera flower extract and its antimicrobial applications. Int. J. Vet. Sci. 6, 286–295.

Kelly, K.L., Coronado, E., Zhao, L.L., Schatz, G.C., 2003. The optical properties of metal nanoparticles: the influence of size, shape, and dielectric environment. J. Phys. Chem. B 107, 668–677. https://doi.org/10.1021/jp026731y.

Kolya, H., Maiti, P., Pandeyand, A., Tripathy, T., 2015. Green synthesis of silver nanoparticles with antimicrobial and azo dye (Congo red) degradation properties using *Amaranthus gangeticus* Linn leaf extract. J. Anal. Sci. Technol. 6, 33. https://doi.org/10.1186/s40543-015-0074-1.

Lee, K.S., El-Sayed, M.A., 2006. Gold and silver nanoparticles in sensing and imaging: sensitivity of plasmon response to size, shape, and metal composition. J. Phys. Chem. B 110, 19220–19225.

Lopez-Miranda, J.L., Vazquez, M., Fletes, N., Esparza, R., Rosas, G., 2016. Biosynthesis of silver nanoparticles using a *Tamarix gallica* leaf extract and their antibacterial activity. Mater. Lett. 176, 285–289. https://doi.org/10.1016/j.matlet.2016.04.126.

Mandal, D., Bolander, M.E., Mukhopadhyay, D., Sarkar, G., Mukherjee, P., 2006. The use of microorganisms for the formation of metal nanoparticles and their application. Appl. Microbiol. Biotechnol. 69, 485–492. https://doi.org/10.1007/s00253-005-0179-3.

Mani, M., Harikrishnan, R., P. Purushothaman, S. Pavithra, P. Rajkumar, S. Kumaresan, Dunia A. Al Farraj, Mohamed Soliman Elshikh, Balamuralikrishnan Balasubramanian, K. Kaviyarasu, Systematic green synthesis of silver oxide nanoparticles for antimicrobial activity, Environ. Resear. 202, 2021a, 111627, https://doi.org/10.1016/j.envres.2021.111627.

Mani, M., Okla, M.K., Selvaraj, S., Ram Kumar, A., Kumaresan, S., Muthukumaran, A., Kaviyarasu, K., El-Tayeb, M.A., Elbadawi, Y.B., Almaary, K.S., Almunqedhi, B.M.A., Elshikh, M.S., 2021b. A novel biogenic Allium cepa leaf mediated silver nanoparticles for antimicrobial, antioxidant, and anticancer effects on MCF-7 cell line. Environ. Resear. 198, 111199.

Mani, M., Pavithra, S., Mohanraj, K., Kumaresan, S., Alotaibi, S.S., Eraqi, M.M., Gandhi, A.D., Babujanarthanam, R., Kaviyarasu, K., Maaza, M., 2021. Studies on the spectrometric analysis of metallic silver nanoparticles (Ag NPs) using Basella alba leaf for the antibacterial activities Environ. Resear 199, 111274. https://doi.org/10.1016/j.envres.2021.111274.

Yamanaka, M., Hara, K., Kudo, J., 2005. Bactericidal actions of a silver ion solution on Escherichia coli, studied by energy-filtering transmission electron microscopy and proteomic analysis. Appl Environ Microbiol. 71 (11), 7589–7593. https://doi.org/10.1128/AEM.71.11.7589-7593.2005.

Nithiyavathi, R., John Sundaram, S., Theophil Anand, G., D. Raj Kumar, A. Dhayal Raj, Dunia A. Al Farraj, Reem M. Aljowaie, Mohamed Ragab AbdelGawwad, Y. Samson, K. Kaviyarasu, Gum mediated synthesis and characterization of CuO nanoparticles towards infectious disease-causing antimicrobial resistance microbial pathogens, J. Infect. Public Health, 14, 2021,1893-1902, https://doi.org/10.1016/j.jiph.2021.10.022.

Nyabola, A.O., Kareru, P.G., Madivoli, E.S., S.I., WanakaiandE.G., Maina,, 2020. J. Inorg. Organomet. Polym. Mater. 30, 3493–3501.

Paramanantham Parasuraman V.T. Anju S.B. Sruthil Lal Alok Sharan K. Siddhardha Busi Mohammed Arshad Kaviyarasu Turki M S. Dawoud Asad Syed Synthesis and antimicrobial photodynamic effect of methylene blue conjugated carbon nanotubes on E. coli and S. aureus Photochem. Photobiol. Sci. 18 2019 563 576.

Paramanantham Parasuraman Asha P Antony, Sruthil Lal S B, Alok Sharan, Busi Siddhardha, Kaviyarasu Kasinathan, Needa A Bahkali, Turki M S Dawoud, Asad Syed, Antimicrobial photodynamic activity of toluidine blue encapsulated in mesoporous silica nanoparticles against Pseudomonas aeruginosa and Staphylococcus aureus Biofouling 35 1 2019 89 103.

Parvataneni, R., 2020. Biogenic synthesis and characterization of silver nanoparticles using aqueous leaf extract of *Scoparia dulcis* L. and assessment of their antimicrobial property. Drug Chem. Toxicol. 43, 307–321. https://doi.org/10.1080/01480545.2018.1505903.

Prasad, T.N.V.K.V., Elumalai, E.K., 2011. Biofabrication of Ag nanoparticles using *Moringa oleifera* leaf extract and their antimicrobial activity. Asian Pac. J. Trop. Biomed. 6, 439–442.

Ramanathan, S., Anbu, P., Lakshmipriya, T., Kasim, F., Lee, C.G., 2018. Eco-friendly synthesis of Solanum trilobatum extract-capped silver nanoparticles is compatible with good antimicrobial activities. J Mol. Struct. 1160, 80–91. https://doi.org/10.1016/j.molstruc.2018.01.056.

Shahverdi, A.R., Fakhimi, A., Shahverdi, H.R., Minaian, S., 2007. Synthesis and effect of silver nanoparticles on the antibacterial activity of different antibiotics against *Staphylococcus aureus* and *Escherichia coli*. Nanomedicine 3 (2), 168–171. https://doi.org/10.1016/j.nano.2007.02.001.

Saratale, R.G., Benelli, G., Kumar, G., Kim, D.S., Saratale, G.D., 2018. Bio-fabrication of silver nanoparticles using the leaf extract of an ancient herbal medicine, dandelion (*Taraxacum officinale*), evaluation of their antioxidant, anticancer potential, and antimicrobial activity against phytopathogens. Environ. Sci. Pollut. Res. 25, 10392–10406.

Sathiyaraj, S., Suriyakala, G., Gandhi, A.D., Babujanarthanam, R., Almaary, K.S., Tse-Wei, C., Kaviyarasu, K., 2021. Biosynthesis, characterization, and antibacterial activity of gold nanoparticles. J. Infect. Pubic Health 14 (12), 1842–1847.

Tripathy, A., Raichur, A.M., Chandrasekaran, N., Prathna, T.C., Mukherjee, A., 2010. Process variables in biomimetic synthesis of silver nanoparticles by aqueous extract of *Azadirachta indica* (Neem) leaves. J. Nanopart Res. 12, 237–246. https://doi.org/10.1007/s11051-009-9602-5.

Vijayan, R., Joseph, S., Mathew, B., 2017. Indigofera tinctoria leaf extract mediated green synthesis of silver and gold nanoparticles and assessment of their anticancer, antimicrobial, antioxidant and catalytic properties. Artif Cells Nanomed. Biotechnol. 46, 861–871. https://doi.org/10.1080/21691401.2017.1345930.

Vijay Kumara, P.P.N., Pammib Pratap Kolluc, S.V.N., Satyanaray, K.V.V., Shameem, U., 2014. Green synthesis and characterization of silver nanoparticles using Boerhaavia diffusa plant extract and their anti bacterial activity 52, 562–566.

Vijilvani, C., Bindhu, M.R., Frincy, F.C., Mohamad, S.A., Sabitha, S., Saravanakumar, K., Devanesan, S., Umadevi, M., Mamduh, J.A., Atif, M., 2019. Antimicrobial and catalytic activities of biosynthesized gold, silver and palladium nanoparticles from Solanum nigurum leaves. J. Photochem. Photobiol. B. 202, 111713.

West, A.R., 1974. Solid State Chemistry and Its Applications. Wiley, New York.

Yoon, K.Y., Hoon Byeon, J., Park, J.H., Hwang, J., 2007. Susceptibility constants of Escherichia coli and Bacillus subtilis to silver and copper nanoparticles. Sci. Total Environ. 373 (2–3), 572–575. https://doi.org/10.1016/j.scitotenv.2006.11.007.

Qi, Z., Zhou, H., Matsuda, N., Honma, I., Shimada, K., Akiko, T., Kato, K., 2004. Characterization of Gold Nanoparticles Synthesized Using Sucrose by Seeding Formation in the Solid Phase and Seeding Growth in Aqueous Solution. J. Phys. Chem. B. 108 (22), 7006–7011. https://doi.org/10.1021/jp035972i.